

# Brain Parcellation Survey Data Reference Manual

Salim Arslan<sup>1,\*</sup>

<sup>1</sup>Biomedical Image Analysis Group, Department of Computing, Imperial College London, London, UK

\*name.surname@imperial.ac.uk

## ABSTRACT

This document provides vital information about how to make the most of the parcellations included in the brain parcellation survey, **Human Brain Mapping: A Systematic Comparison of Brain Parcellation Methods for Human Cerebral Cortex**<sup>1</sup>, in which a large-scale and systematic comparison is carried out between 10 subject-level and 24 groupwise parcellations, either derived in a data-driven fashion using resting-state functional connectivity or obtained from publicly available resources. All the parcellations evaluated in this study are gathered together for the use of other researchers at: <https://biomedica.doc.ic.ac.uk/brain-parcellation-survey/>. It may be beneficial to read this manual for better understanding the parcellation data (including the directory structure and file names) as well as learning more about the implementation details and processing decisions made throughout this study. Some scripts and code snippets are also provided to load and visualise the parcellation data in MATLAB and Python. The evaluation code is also made publicly available for the use of other researchers at: <https://github.com/sarslancs/parcellation-survey-eval>.

## 1 Directory Structure

If you have downloaded the parcellations all at once from the Imperial College London data storage, you should have the following directory structure, after having extracted the zip file.

```
/
├── Subject
│   ├── Arslan
│   │   ├── 100307_Arslan_1_L.mat
│   │   ├── ...
│   │   └── ...
│   └── ...
├── Group
│   ├── AAL
│   │   ├── AAL.L.mat
│   │   ├── ...
│   │   └── ...
│   └── ...
├── Scripts
├── dataset1.txt
└── dataset2.txt
```

- **Subject:** Subject-level parcellations are located in this folder.
- **Group:** Connectivity-driven and publicly available groupwise parcellations are located in this folder.
- **Scripts:** This folder includes several scripts for loading/viewing parcellations in MATLAB and Python.
- `dataset{1,2}.txt`: IDs of the subjects constituting Dataset 1 and Dataset 2.

## 2 File Names

Subject-level parcellation files are in one of the following formats:

- `<subjectID>_<name>_<session>_<hemisphere>.mat`, if two parcellations are available for a method (this is the case for connectivity-driven methods, in which two parcellations are computed from two sets of BOLD timeseries per subject), e.g. `100307_Arslan_1_L.mat`.
- `<subjectID>_<name>_<hemisphere>.mat`, if only one parcellation is available for a method (this is the case for the publicly available parcellations), e.g. `100307_Desikan_R.mat`.

Group-level parcellation files are in one of the following formats:

- `<name>_<dataset>_<hemisphere>.mat`, if two parcellations are computed for a method (this is the case for connectivity-driven methods, where one parcellation is computed from Dataset 1 and one from Dataset 2), e.g. `100307_Arslan_1_L.mat`.
- `<name>_<hemisphere>.mat`, if only one parcellation is available for a method (this is the case for the publicly available parcellations), e.g. `Gordon_L.mat`.

### 3 Parcellation Data

Each `mat` file is packed with the actual parcellations and additional data structures, described as follows:

- `parcels`: An  $N \times k$  matrix, where  $N$  denotes the number of vertices and  $k$  is the number of available parcellations for that method/subject.  $N$  is always equal to 29696 for the left (L) and 29716 for the right (R) hemisphere.  $k$  varies depending on the number of parcellations computed or available for a method/subject.
- `resolution`: A  $1 \times k$  vector that shows the number of cortical regions at each resolution.
- `neighs`: A  $1 \times k$  cell structure, in which each cell contains a  $K \times K$  adjacency matrix, where  $K$  denotes the parcellation resolution. An adjacency matrix provides the 'neighbourhood' information which might be required to inject spatial constraints to connectivity networks derived from the provided parcellations. Here, two parcels  $A$  and  $B$  are considered as neighbours, or adjacent, if vertices  $v_i \in A$  and  $v_j \in B$  are directly connected by an edge in the cortical mesh.

### 4 Load Parcellations in MATLAB and Python

`load_all_group_parcellations.m`, `py` and `load_all_single_subject_parcellations.m`, `py` are located in the `Scripts` folder and can be used for loading the parcellations in an iterative manner either in MATLAB or Python. Please see the comments in each script for further information.

### 5 How to View Parcellations?

`view_parcellation.m` allows you to visualise a parcellation directly in MATLAB, by projecting it (or any 1D cortical data) onto one of the given surfaces (`pial`, `white`, `midthickness`, `inflated`, `very_inflated`, and `sphere`). The script as well as the surfaces and the GIFTI toolbox<sup>1</sup> (required for visualisation) are located in the `Scripts` folder. Simply run the following code snippet to plot any of the provided parcellations as in Figure 1.

```
load('Arslan_1_L.mat', 'parcels');
parc = parcels(:,4); % K = 100
view_parcellation(parc, 'L', 'inflated');
```

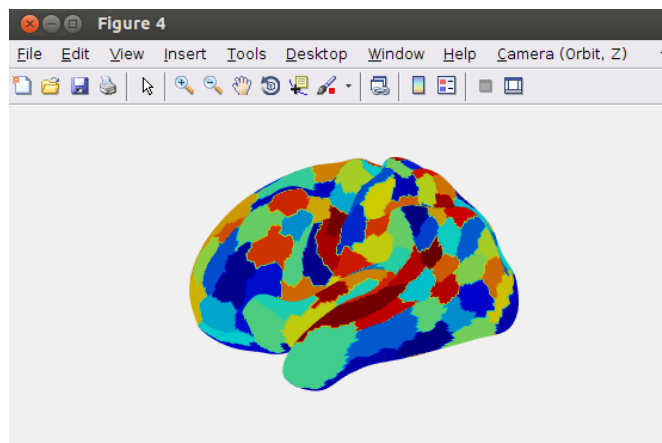


**Figure 1.** Viewing a parcellation in MATLAB.

<sup>1</sup> <http://www.artefact.tk/software/matlab/gifti/>

## 6 Evaluation Code

Scripts/functions used to carry out the experiments for the evaluation of parcellations with respect to reproducibility, clustering validity, and agreement with other modalities are made publicly available at <https://github.com/sarslancs/parcellation-survey-eval>. If you have downloaded the parcellation data from the survey page, you can also find a copy of each script in the `eval` folder under `Scripts`. Please see in-file instructions/comments to run them. Unfortunately, source code for the network analysis part of the pipeline is currently not online, but this may change in the future. So stay tuned!

## 7 Parcellation Methods: Implementation Details

This section briefly summarises the methodology behind each parcellation method, with an emphasis on the implementation details and processing decisions followed in the paper.

### 7.1 Subject-Level Methods

#### Arslan<sup>2</sup>

A two-level approach that combines k-means with hierarchical clustering. Initially, each hemisphere is parcellated into a set of 1000 supervertices using a method inspired by the SLIC superpixels<sup>3</sup>. At the second level, a hierarchical tree is constructed using Ward's linkage rule<sup>4</sup> with Euclidean distance and parcellations for varying number of clusters are obtained by cutting this tree at different levels.

A critical parameter in this approach is the  $m$  parameter that relatively weighs functional homogeneity and spatial contiguity of the regions in the distance function. We experimentally set this parameter to 0.7. Our experiments revealed that lower values tend to produce more regular shaped clusters, but at the cost of obtaining less homogeneous supervertices. Greater values of  $m$  help cluster more similar vertices together, but the spatial coherency of supervertices is severely affected, reducing the reproducibility of the final parcels.

#### Blumensath<sup>5</sup>

A two-level method that combines region growing and hierarchical clustering. Each seed vertex is grown into a region (initial cluster) by an iterative process in which vertices are attached to a region based on their similarity with the neighbouring regions. After all vertices have been assigned to a cluster, final parcels are obtained by merging adjacent clusters using hierarchical clustering with Ward's linkage rule<sup>4</sup> and the Euclidean distance, same as in *Arslan*. However, this approach differs from *Arslan* in two ways. (1) Instead of relying on a fixed number of seed vertices to start the parcellation process, it automatically locates highly homogeneous cortical regions that can be used to compute seed vertices. (2) Instead of using the average timeseries within a cluster for representation, the average signal is computed from the immediate neighbourhood of a ROI centred at each cluster's seed vertex.

In the process of region growing, each vertex is correlated with the regions to which they are spatially adjacent. In order to assign a vertex to a cluster, the correlation between the vertex' timeseries and the regions' timeseries should exceed  $p$  times the maximal correlation between all other region timeseries and their associated neighbourhood vertex timeseries. Based on our observations and the discussion in the original paper, we set this parameter to 0.9, which significantly increased the computational speed of the approach with only a minimal impact on the final parcellations.

#### Bellec<sup>6</sup>

A region growing approach that maximizes homogeneity of parcellations, in which homogeneity is defined as the average correlation between the timeseries associated with any pair of vertices within a region. Since this method is driven by homogeneity, a size constraint ( $t$ ) should be imposed in order to avoid having heterogeneous parcellations in terms of parcel size (e.g. having many small, highly homogeneous parcels with a few very large parcels across the cortex). To this end, for each parcellation resolution we set the size parameter to the expected average parcel size (i.e. number of vertices / number of parcels). During the region growing process, regions that exceed the size parameter  $t$  are validated and excluded from further consideration. This ensures that the size of a validated region (i.e. a parcel) cannot exceed  $(2t - 2)$ , as it is possible that two regions of size  $(t - 1)$  can still be merged during the growing process. Different from the original paper, we specify the number of regions beforehand; hence the algorithm keeps merging the smallest adjacent regions until the desired resolution has been reached.

#### K-Means<sup>7</sup>

The well-known  $k$ -means clustering algorithm is used to compute parcellations for varying number of parcels. In order to reduce the computational cost, we followed the instructions in<sup>7</sup> and reduced the dimensionality of the timeseries data of each subject to 500 components via PCA, capturing about 50% of the variance.  $k$ -means naturally does not guarantee spatial contiguity,

as the algorithm is just designed to minimise the sum of squared differences between the timeseries and their associated cluster centroids. To enforce spatial contiguity within parcels, we concatenated the spatial coordinates of each vertex as extra dimensions to the PCA components. Similar to SLIC-supervoxels as defined in<sup>2</sup>, a parameter is used to relatively weight the connectivity data (PCA components) and the spatial coordinates. We set this parameter to 0.75, as higher values resulted in extremely disjoint parcellations, in which many parcels consisted of spatially distant sub-regions, whereas lowering the parameter yielded parcellations dominated by spatial proximity, rather than similarity in functional connectivity.

#### **Ward<sup>4</sup> (Agglomerative hierarchical clustering)**

We join vertices into non-overlapping parcels using another popular clustering algorithm, agglomerative hierarchical clustering with Ward's linkage rule<sup>4</sup>. This approach builds a hierarchy of clusters using a bottom-up strategy in which pairs of clusters are merged if the similarity of their timeseries is the maximal among the other pairing clusters. We only join adjacent clusters into a higher level in order to ensure the spatial contiguity throughout the parcellation process. The algorithm is driven by Ward's linkage rule and the similarity between pairing clusters is computed by the Euclidean distance. The algorithm iteratively constructs a dendrogram, in which the leaves represent the vertices and the root represents an entire hemisphere. Cutting this tree at different levels of depth produces parcellations with the desired precision. Different from *Arslan* and *Blumensath*, this method directly runs on the timeseries data, instead of relying on an initial fine-resolution parcellation.

#### **N-Cuts<sup>8</sup> (Spectral clustering with normalised cuts)**

A spectral clustering technique based on normalised cuts is applied to the connectivity data as described in<sup>8</sup>. An affinity matrix  $W$  is built by cross-correlating vertices with each other. In order to obtain spatially contiguous parcellations, we only retain the edges constructed between adjacent vertices and discard the others. After ensuring that the resulting affinity matrix is fully-connected and positive-semidefinite (i.e. all  $W_{ij} \geq 0$ ), we apply spectral decomposition to the normalised graph Laplacian, defined as  $L = D^{-1/2}(D - W)D^{-1/2}$ , where  $D$  is a diagonal matrix with each entry  $D_{ii} = \sum_j W_{ij}$  representing the degree of vertex  $i$ . By discretising<sup>9</sup> the eigenvectors obtained via this decomposition, we compute the final parcellations.

#### **Random<sup>10</sup>**

To have a baseline for measuring the performance of the connectivity-driven approaches, we obtained random parcellations by using Poisson disk sampling as described in<sup>10</sup>. This is achieved by sub-dividing the cortical mesh into roughly evenly-sized parcels based on Poisson disk sampling.

#### **Geometric<sup>7</sup>**

To have another baseline for measuring the performance of the connectivity-driven approaches, we obtained "geometric" parcellations by applying k-means clustering to the spatial vertex coordinates as described in<sup>7</sup>. To this end, we use coordinates as projected onto the "midthickness" cortical surface, which is a geometrically close surface to the human cerebral cortex. Since the parcellation is directly driven by spatial proximity between cortical vertices, it is likely to obtain regularly shaped parcels, with roughly similar size.

#### **Destrieux<sup>11</sup>**

A cortical atlas provided as part of the HCP datasets. It is an anatomical parcellation that subdivides the cerebral cortex with respect to the limit between the gyral and sulcal regions, determined by the curvature of the surface. It subdivides the cerebral cortex into a fixed number of 75 parcels per hemisphere.

#### **Desikan<sup>12</sup>**

A cortical atlas provided as part of the HCP datasets. It offers an anatomical parcellation based on the gyri, where a gyrus is defined as the part visible on the pial surface, limited by the adjacent banks of the sulci. It subdivides the cerebral cortex into a fixed number of 35 parcels per hemisphere.

## **8 Group-Level Methods**

### **Arslan**

A group-level parcellation is obtained from the subject-level *Arslan* parcellations using the 2-level approach.

### **Blumensath**

A group-level parcellation is obtained from the subject-level *Blumensath* parcellations using the 2-level approach.

### **Bellec**

A group-level parcellation is obtained from the subject-level *Bellec* parcellations using the 2-level approach.

## **k-means clustering**

*K-Means-2*: A group-level parcellation is obtained from the subject-level *K-Means* parcellations using the 2-level approach.

*K-Means-AVR*: k-means clustering is applied to the group average matrix to obtain a groupwise parcellation for varying resolutions. To generate more spatially contiguous parcels, we concatenate the average spatial coordinates with the group average matrix. Similar to its subject-level counterpart, a parameter is used to relatively weight the connectivity data and spatial coordinates. We set this parameter to 0.75, which yield highly homogeneous parcellations while maintaining the spatial contiguity to some extent.

## **Hierarchical clustering**

*Ward-2*: A group-level parcellation is obtained from the subject-level *Ward* parcellations using the 2-level approach.

*Ward-AVR*: Group average matrix is fed into an agglomerative hierarchical clustering algorithm using the same setting as in the subject-level *Ward* parcellations.

## **Spectral clustering with normalised cuts**

*N-Cuts-2*: A groupwise parcellation is obtained from the subject-level *N-Cuts* parcellations using the 2-level approach.

*N-Cuts-AVR*: We obtained a temporal correlation matrix from the group average matrix as described in<sup>13</sup> and converted that into a spatially-constrained affinity matrix by only retaining the edges between adjacent vertices. By applying the same processing steps as in its subject-level counterpart, we compute groupwise parcellations for different resolutions.

## **Geometric parcellations**

k-means clustering of the average “midthickness” coordinates as described in<sup>7</sup>.

## **Gordon<sup>14</sup>**

A publicly available parcellation is computed from a group of 120 healthy young adults using resting-state functional connectivity. Boundary maps are generated from the gradients computed across the average functional connectivity matrices and fed into a surface-based watershed segmentation algorithm to obtain final parcellations. In our experiments we use the parcellation provided by the original developers of the method (<http://www.nil.wustl.edu/labs/petersen/Resources.html>). In this parcellation, cortical areas close to parcel boundaries are discarded as they are assumed to be the locations where the connectivity abruptly changes. To be consistent with the other parcellations in our experiments, we slightly dilate each parcel such that the parcellation covers the entire cortical surface.

## **Power<sup>15</sup>**

This method attempts to identify functionally active groups of vertices (communities) that are consistent with the known structures in the brain using resting-state functional connectivity. Based on their analysis, a whole-brain parcellation is proposed including several resting-state networks (RSN) identified across many subjects. We used the version of this parcellation distributed by Balsa (<https://balsa.wustl.edu/study/show/WG33>), which was subject to a volume-to-surface sampling. The RSNs were projected onto the cortical surface and preprocessed for filling the holes emerged during the sampling process. These clusters are further subdivided into spatially contiguous parcels. As a post process, we remove very small parcels (that contain fewer than 25 vertices) from the parcellation and dilate the remaining parcels to adjust for the lost vertices.

## **Yeo<sup>16</sup>**

Similar to Power, this method identifies functionally coupled regions (or resting-state networks) that spawn across the cerebral cortex. Functional connectivity data from 1000 healthy subjects is subdivided into 7 and 17 clusters using a GMM-based clustering approach. In our experiments, we use the 17-cluster parcellation provided by Balsa (<https://balsa.wustl.edu/study/show/WG33>) and further subdivide clusters into spatially contiguous parcels. We finally remove very small parcels (that contain fewer than 25 vertices) from the parcellation and apply dilation for hole-filling.

## **ICA**

Group-average parcellations by means of group-ICA<sup>17</sup> are obtained at several different dimensionalities (25, 50, 100, 200, 300), using a group-PCA output generated from the HCP S500 subjects (only 468 subjects were used) with MIGP (MELODIC’s Incremental Group-PCA)<sup>13</sup> and made publicly available as part of the S500 release ([https://db.humanconnectome.org/data/projects/HCP\\_500](https://db.humanconnectome.org/data/projects/HCP_500)). This output provides a very close approximation to the PCA components applied to the concatenation of all subjects’ timeseries. Connected components within each ICA parcel are relabelled to obtain spatially contiguous parcellations. We finally remove very small parcels (that contain fewer than 25 vertices) from the parcellations and apply dilation to the remaining parcels to adjust for the lost vertices.

### **Destrieux<sup>11</sup>**

Surface-based parcellations provided by the HCP maintain parcel-wise correspondence across subjects. Therefore, we only applied majority voting to subject-level *Destrieux* parcellations to obtain a groupwise representation.

### **Desikan<sup>12</sup>**

Similarly to *Destrieux*, majority voting is used to generate the groupwise *Desikan* atlas.

### **Baldassano<sup>18</sup>**

A multi-purpose clustering algorithm based on non-parametric Bayesian modelling designed for identifying locally-connected, spatially-contiguous clusters is applied to the group-PCA output<sup>13</sup> of 468 subjects provided by the HCP S500 release. In our experiments we use the 172-parcel atlas provided by the original developers of the method (<http://www.princeton.edu/~chrisb/code.html>).

### **Automated Anatomical Labeling (AAL)<sup>19</sup>**

This is an anatomical atlas labelled with respect to landmarks following the sulci course on the brain that can be obtained from [http://www.gin.cnrs.fr/AAL2\\_files/aal2\\_for\\_SPM12.tar.gz](http://www.gin.cnrs.fr/AAL2_files/aal2_for_SPM12.tar.gz). Although it was generated from a single subject's brain, it is one of the widely used atlases for network analysis.

In order to obtain surface-based parcellations from AAL, we use volume-to-surface and surface-to-surface sampling techniques to project volumetric parcels onto the HCP average cortical atlas (Conte69)<sup>20</sup>. The volume-to-surface projection is achieved by using FreeSurfer's `mri_vol2surf` method<sup>21</sup>. The volumetric labels are re-sampled to the reconstructed Colin27 surface<sup>22</sup> by using a registration matrix between the Colin27 and the SPM's single-subject T1 images (<http://www.fil.ion.ucl.ac.uk/spm/software/spm12/>), both of which belong to the same subject. The SPM single-subject T1 image was originally used to obtain the AAL atlas, hence almost all cortical labels can be projected with minimal error.

We transform the cortical labels from the Colin27 surface onto the Conte69 atlas, by using Multimodal Surface Matching (MSM), a tool for registering cortical surfaces<sup>23</sup>. We first use MSM's `msmapplywarp` function to obtain a "warped" spherical mesh of the Colin27 surface by the guidance of one of the HCP subjects' native spherical surface, as both are in the FreeSurfer space. Driven by this warped mesh, we then re-sample the cortical labels from the original surface to the Conte69 surface using the `msmresample` method. In order to fill the holes that may have emerged during the sampling process, dilation is applied to each parcel. Unfortunately, volume-to-surface re-sampling is not a straightforward process, and hence, it is impossible to retain all volume-based parcels after projection. However, we ensured the parcellation boundaries and relative positions of parcels to each other were as faithful to the original atlas as possible.

### **Shen<sup>24</sup>**

A spectral clustering approach that computes a groupwise parcellation driven by an optimisation process that guarantees functional homogeneity within each region and ensures that computed parcels are highly consistent across subjects. In order to incorporate this parcellation into our experiments, we project the volumetric parcellation provided by the developers of the method ([http://www.nitrc.org/frs/?group\\_id=51](http://www.nitrc.org/frs/?group_id=51)) to the HCP average cortical surface<sup>20</sup>. To this end, we follow a similar pipeline as described above. Since the publicly available 1 mm volumetric parcellations are in the same space as the Colin27 brain, the volumetric labels can be effectively obtained using the same algorithmic steps. In order to fill holes that may have emerged during the sampling process, dilation is applied to each parcel.

### **Fan<sup>25</sup>**

A whole brain parcellation is obtained using both anatomical features and connectivity-driven information. First, the brain is subdivided into anatomically distinct parcels using the Desikan atlas<sup>12</sup>. Each anatomical region is further parcellated into sub-regions using functional and structural connectivity data from 40 healthy subjects provided by the HCP. As the parcellation is generated from the HCP datasets, an HCP-compatible volumetric atlas is already available (<http://atlas.brainnetome.org/>). To project these volumetric parcels onto the surface, we just utilize the HCP `wb_command -volume-to-surface-mapping` method after masking out the sub-cortical labels. In order to fill the holes that may have emerged during the sampling process, dilation is applied to each parcel.

### **GRASP<sup>26</sup>**

A method based on Markov Random Field (MRF) that can subdivide the cortex into spatially contiguous parcels by using shape priors. We use the code provided by the developer of the approach (<https://www.cbica.upenn.edu/sbia/software/grasp/index.html>) to generate a groupwise parcellation using our group average matrix. In order to compensate for the computational cost, we run the method in the hierarchical clustering mode. That is, we first over-parcellate the cortical surface into 10000 initial clusters, and obtain final parcellations from this low-dimensional matrix. The method



does not directly allow specifying the resolution of the parcellation; hence we obtain parcellations for different number of clusters by tuning the label-cost parameter based on the discussion in the paper.

### **GRAMPA<sup>27</sup>**

An MRF model that iteratively updates parcel centres and parcel assignments based on modality specific costs. The parcellation is computed from the group average matrix using an in-house implementation.

### **JOINT<sup>28</sup>**

A multi-layer graph is jointly constructed with respect to the connectional similarity within and between subjects and spectral decomposition of this joint graph is used to cluster each cortical vertex into a region in order to obtain whole-brain groupwise parcellations. We used an in-house implementation of this method to obtain parcellations. Different from the original paper, we reduce the spatial dimensionality of the cortical surface down to 2000 regions using SLIC-based supervoxel clustering<sup>2</sup> in order to reduce computational cost, and hence, to run the method for all subjects in our dataset.

### **Glasser<sup>29</sup>**

A semi-automated multi-modal parcellation that is delineated using features from several modalities, including but not limited to function, connectivity, cortical architecture, and topography. It also incorporates expert knowledge and meta-analysis results from the literature in order to delineate boundaries between cortical regions with high precision. In our experiments, we used the parcellation computed by using data from 210 healthy subjects, which has been made publicly available by the developers (<https://balsa.wustl.edu/study/show/RVVG>).

## **References**

1. Arslan, S. *et al.* Human brain mapping: A systematic comparison of brain parcellation methods for human cerebral cortex. *NeuroImage* (2017).
2. Arslan, S. & Rueckert, D. Multi-level parcellation of the cerebral cortex using resting-state fMRI. In Ourselin, S., Alexander, D., Westin, C.-F. & Cardoso, M. (eds.) *MICCAI 2015 LNCS*, 47–54 (2015).
3. Achanta, R. *et al.* Slic superpixels compared to state-of-the-art superpixel methods. *IEEE transactions on pattern analysis machine intelligence* **34**, 2274–2282 (2012).
4. Ward, J. H. Hierarchical grouping to optimize an objective function. *J. Am. statistical association* **58**, 236–244 (1963).
5. Blumensath, T. *et al.* Spatially constrained hierarchical parcellation of the brain with resting-state fMRI. *NeuroImage* **76**, 313–324 (2013).
6. Bellec, P. *et al.* Identification of large-scale networks in the brain using fmri. *NeuroImage* **29**, 1231–1243 (2006).
7. Thirion, B., Varoquaux, G., Dohmatob, E. & Poline, J. B. Which fMRI clustering gives good brain parcellations? *Front Neurosci* **8**, 167 (2014).
8. Craddock, R. C., James, G. A., Holtzheimer, P. E., Hu, X. P. & Mayberg, H. S. A whole brain fMRI atlas generated via spatially constrained spectral clustering. *Hum Brain Mapp* **33**, 1914–1928 (2012).
9. Yu, S. X. & Shi, J. Multiclass spectral clustering. In *Computer Vision, 2003. Proceedings. Ninth IEEE International Conference on*, 313–319 (IEEE, 2003).
10. Schirmer, M. D. *Developing brain connectivity: effects of parcellation scale on network analysis in neonates*. Ph.D. thesis, King's College London (2015).
11. Fischl, B. *et al.* Automatically parcellating the human cerebral cortex. *Cereb. cortex* **14**, 11–22 (2004).
12. Desikan, R. S. *et al.* An automated labeling system for subdividing the human cerebral cortex on mri scans into gyral based regions of interest. *NeuroImage* **31**, 968–980 (2006).
13. Smith, S. M., Hyvärinen, A., Varoquaux, G., Miller, K. L. & Beckmann, C. F. Group-pca for very large fmri datasets. *NeuroImage* **101**, 738–749 (2014).
14. Gordon, E. M. *et al.* Generation and evaluation of a cortical area parcellation from resting-state correlations. *Cereb. Cortex* **26**, 288–303 (2016). DOI 10.1093/cercor/bhu239.
15. Power, J. D. *et al.* Functional network organization of the human brain. *Neuron* **72**, 665–678 (2011).
16. Yeo, B. T. T. *et al.* The organization of the human cerebral cortex estimated by intrinsic functional connectivity. *J Neurophysiol* **106**, 1125–1165 (2011). DOI 10.1152/jn.00338.2011.

17. Beckmann, C. F. & Smith, S. M. Probabilistic independent component analysis for functional magnetic resonance imaging. *IEEE Trans Med Imag* **23**, 137–152 (2004).
18. Baldassano, C., Beck, D. M. & Fei-Fei, L. Parcellating connectivity in spatial maps. *PeerJ* **3**, e784 (2015).
19. Tzourio-Mazoyer, N. *et al.* Automated anatomical labeling of activations in SPM using a macroscopic anatomical parcellation of the MNI MRI single-subject brain. *NeuroImage* **15**, 273–289 (2002). DOI <http://dx.doi.org/10.1006/nimg.2001.0978>.
20. Van Essen, D. C., Glasser, M. F., Dierker, D. L., Harwell, J. & Coalson, T. Parcellations and hemispheric asymmetries of human cerebral cortex analyzed on surface-based atlases. *Cereb. Cortex* **22**, 2241–2262 (2012).
21. Fischl, B. Freesurfer. *NeuroImage* **62**, 774–781 (2012).
22. Holmes, C. J. *et al.* Enhancement of mr images using registration for signal averaging. *J. computer assisted tomography* **22**, 324–333 (1998).
23. Robinson, E. C. *et al.* MSM: A new flexible framework for multimodal surface matching. *NeuroImage* **100**, 414–426 (2014).
24. Shen, X., Tokoglu, F., Papademetris, X. & Constable, R. T. Groupwise whole-brain parcellation from resting-state fmri data for network node identification. *NeuroImage* **82**, 403–415 (2013).
25. Fan, L. *et al.* The human brainnetome atlas: A new brain atlas based on connectional architecture. *Cereb. Cortex* bhw157 (2016).
26. Honnorat, N. *et al.* Grasp: geodesic graph-based segmentation with shape priors for the functional parcellation of the cortex. *NeuroImage* **106**, 207–221 (2015).
27. Parisot, S., Glocker, B., Schirmer, M. D. & Rueckert, D. GraMPa: Graph-based multi-modal parcellation of the cortex using fusion moves. In *MICCAI 2016 LNCS* (2016).
28. Arslan, S., Parisot, S. & Rueckert, D. Joint spectral decomposition for the parcellation of the human cerebral cortex using resting-state fMRI. In Navab, N., Hornegger, J., Wells, W. M. & Frangi, A. F. (eds.) *IPMI 2015 LNCS*, 85–97 (2015).
29. Glasser, M. *et al.* A multi-modal parcellation of human cerebral cortex. *Nat.* (2016).